Molecular Cancer Therapeutics

MOR209/ES414, a Novel Bispecific Antibody Targeting PSMA for the Treatment of Metastatic Castration-Resistant Prostate Cancer

Gabriela Hernandez-Hoyos, Toddy Sewell, Robert Bader, Jeannette Bannink, Ruth A. Chenault, Mollie Daugherty, Maria Dasovich, Hang Fang, Rebecca Gottschalk, John Kumer, Robert E. Miller, Padma Ravikumar, Jennifer Wiens, Paul A. Algate, David Bienvenue, Catherine J. McMahan, Sateesh K. Natarajan, Jane A. Gross, and John W. Blankenship

Abstract

Treatment of metastatic, castration-resistant prostate cancer (mCRPC) remains a highly unmet medical need and current therapies ultimately result in disease progression. Immunotherapy is a rapidly growing approach for treatment of cancer but has shown limited success to date in the treatment of mCRPC. We have developed a novel humanized bispecific antibody, MOR209/ES414, built on the ADAPTIR (modular protein technology) platform, to redirect T-cell cytotoxicity toward prostate cancer cells by specifically targeting T cells through CD3ε to prostate cancer cells expressing PSMA (prostate-specific membrane antigen). *In vitro* cross-linking of T cells with PSMA-expressing tumor cells by MOR209/ES414 triggered potent target-dependent tumor lysis and induction of target-dependent T-cell activation and proliferation. This activity occurred at low picomolar concentrations of MOR209/ES414 and was effective at low T-effector to tumor target cell ratios. In addition, cytotoxic activity was equivalent over a wide range of PSMA expression on target cells, suggesting that as few as 3,700 PSMA receptors per cell are sufficient for tumor lysis. In addition to high sensitivity and *in vitro* activity, MOR209/ES414 induced limited production of cytokines compared with other bispecific antibody formats. Pharmacokinetic analysis of MOR209/ES414 demonstrated a serum elimination half-life in NOD/SCID γ (NSG) mice of 4 days. Administration of MOR209/ES414 in murine xenograft models of human prostate cancer significantly inhibited tumor growth, prolonged survival, and decreased serum prostate-specific antigen levels only in the presence of adoptively transferred human T cells. On the basis of these preclinical findings, MOR209/ES414 warrants further investigation as a potential therapeutic for the treatment of CRPC. *Mol Cancer Ther; 1–11. ©2016 AACR.*

Introduction

Prostate cancer is the most common and the second most lethal cancer in men (1). Despite treatment with a combination of surgery, local radiotherapy, and/or androgen deprivation therapy (ADT), cancer relapses in roughly 30% of patients. Patients who relapse after surgery or radiation typically respond to treatment with ADT, but often relapse within several years. Prostate cancer insensitive to ADT is categorized as castration-resistant prostate cancer (CRPC). Although new therapeutics have been approved for treating metastatic CRPC (mCRPC) such as cabazitaxel, abiraterone, and enzalutamide, the overall survival benefit from individual agents is only 2 to 8 months (1–4). A major unmet medical need exists for new therapies that can treat metastatic disease, improve quality of life, and prolong survival (5).

Increased understanding of tumor–host interactions has triggered development of numerous immunotherapies in prostate cancer, including peptide and RNA/DNA vaccines, cell-based vaccines, chimeric antigen receptor modified T cells, T-cell engaging bispecific antibodies, and checkpoint inhibitors (6). The clinical success of immunotherapeutic approaches in prostate cancer has been limited to date, although a number of prostate lineage-specific antigens, such as prostate-specific membrane antigen (PSMA, also known as *FOLH1*), offer potential therapeutic targets. The biology of PSMA and its relevance as a tumor-specific antigen for mCRPC has been reviewed extensively (7–9). PSMA has been used as a target for the development of diagnostics (10) and for therapeutic mAbs (11–14). Bispecific antibody fragments in either a diabody format (15) or a tandem single-chain variable fragment (scFv) format (16) targeting PSMA and the T-cell receptor (TCR) complex subunit CD3ε have been described previously. One of these molecules, BAY2010112, is currently under early clinical evaluation. In preclinical studies, bispecific antibody fragments targeting PSMA and CD3ε have shown potent target-dependent redirection of T-cell cytotoxicity

Emergent BioSolutions, Seattle, Washington.

Note: Supplementary data for this article are available at Molecular Cancer Therapeutics Online (http://mct.aacrjournals.org/).

Current address for J. Wiens: Eurofins Lancaster Laboratories, Inc., Thousand Oaks, CA; current address for P.A. Algate: Theraclone, Seattle, WA; and current address for S.K. Natarajan: Biologics Development Centre, Dr. Reddy's Laboratories Ltd., Hyderabad, Telengana, India.

Corresponding Author: John W. Blankenship, Emergent BioSolutions, 2401 4th Avenue, Suite 1050, Seattle, WA 98121. Phone: 206-859-6612; Fax: 206-838-0503; E-mail: jblankenship@ebsi.com

doi: 10.1158/1535-7163.MCT-15-0242

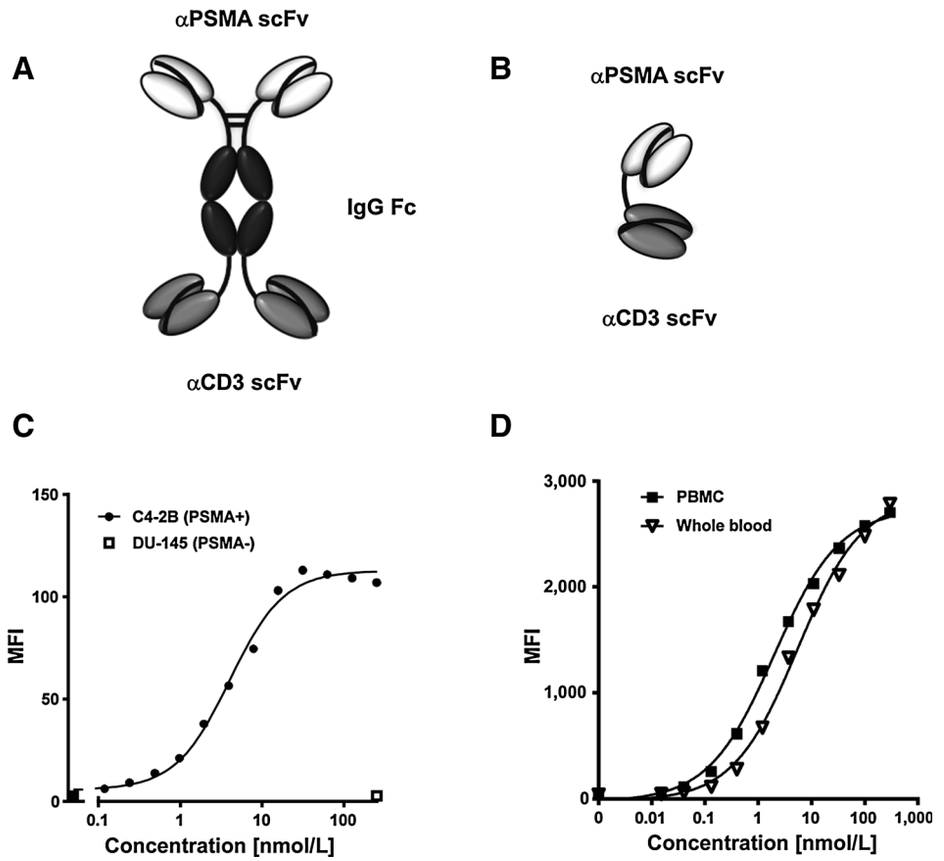

Figure 1.
A, MOR209/ES414 structure. **B,** tandem scFv structure. **C,** binding of MOR209/ES414 on prostate cancer cell lines plotted as median fluorescence intensity (MFI). **D,** binding of MOR209/ES414 on primary human T cells in either a mixed population of PBMC or in whole blood plotted as MFI.

(RTCC) toward prostate cancer cells both *in vitro* and in xenograft models. Although highly active in preclinical studies, these molecules have clinically relevant limitations, including short serum elimination half-lives, requiring daily dosing, and induction of high levels of cytokine release, which can lead to toxicities such as cytokine release syndrome (CRS). In addition, current hypotheses have constrained the variety of bispecific antibodies designed to redirect T-cell cytotoxicity to those with monovalent binding to both targets and limited distance between binding domains (17).

We have developed an alternative bispecific antibody targeting PSMA and CD3ε, MOR209/ES414, using the ADAPTIR platform (Fig. 1). Unlike previously described bispecific antibody fragments, MOR209/ES414 binds bivalently to both PSMA and CD3ε, yet does not cross-link and activate T cells without target present. MOR209/ES414 also incorporates a modified antibody Fc region that improves serum stability but does not cross-link T cells or target cells through Fcγ receptors like CD16 or CD64. Similar to bispecific antibody fragments, MOR209/ES414 induces target-dependent redirection of T-cell cytotoxicity toward prostate cancer cells expressing PSMA *in vitro* and *in vivo*; however, MOR209/ES414 has a prolonged serum elimination half-life compared with bispecific antibody fragments and thus requires less frequent dosing for comparable efficacy in mouse xenograft studies. Notably, MOR209/ES414 shows a reduced cytokine release profile compared with other bispecific antibody formats that can redirect T-cell cytotoxicity, but still drives serial lysis and multiple rounds of T-cell proliferation.

Materials and Methods

Molecular biology and reagent generation

The sequence for MOR209/ES414 is derived from variable domains of two separate murine antibodies specific for PSMA and CD3ε. Immunoglobulin variable regions were converted to single-chain variable fragments (scFv) by adding flexible linker sequences [e.g., $(Gly_4Ser)_3$]. Murine scFv constructs were then humanized by grafting murine complementarity determining regions (CDR) to human frameworks. The MOR209/ES414 ADAPTIR construct was assembled by linking humanized anti-PSMA and anti-CD3ε scFv domains to the N- and C-terminus of human IgG1 Fc. Mutations were introduced to the Fc region to ablate FcγR binding (L234A, L235A, and G237A) and C1q binding (K322A). The final domain order of MOR209/ES414 is anti-PSMA scFv (VLVH)-hinge-CH2-CH3-linker-anti–CD3 scFv (VHVL; Fig. 1A). MOR209/ES414 was expressed as a recombinant single polypeptide in a CHO cell line and purified from cell culture supernatant using affinity chromatography and size exclusion chromatography. The anti-PSMA × anti–CD3 scFv-scFv comparator contains the amino acid sequence of BAY2010112 (16, 18), and was expressed recombinantly using either transient transfection of HEK293 cells or a CHO cell line. Anti-PSMA × anti-CD3 scFv-scFv was purified from cell culture supernatant using IMAC affinity chromatography and size exclusion chromatography; no differences were observed between proteins produced in HEK293 or CHO cells. A control ADAPTIR construct was also assembled by replacing the anti-CD3 scFv in MOR209/ES414 with the anti-CD3 scFv (I2C) found in BAY2010112, and was

expressed recombinantly using transient transfection of HEK293 cells and purified similar to MOR209/ES414.

Cell lines and cell culture

LNCaP, VCaP, DU-145, 22Rv1, and MDA-PCa-2b cell lines were obtained from the ATCC, and were authenticated by short tandem repeat (STR) analysis by the ATCC. A subline of LNCaP-expressing GFP, LNCaP (GFP), was obtained from Anticancer Inc.; no further authentication was done by the authors. Two other sublines of LNCaP, C4-2 and C4-2B, were obtained from the MD Anderson Cancer Center, and were previously authenticated using STR analysis. C4-2B cells were also reauthenticated by STR analysis by General Genetics Corporation. All cell lines, except VCaP and MDA-PCa-2b, were cultured in RPMI-1640 (Life Technologies) with 10% FBS. VCaP cells were cultured in DMEM (Life Technologies) with 10% FBS; and MDA-PCa-2b cells were cultured in BRFF-HPC1 media (Athena Enzyme Systems) with 20% FBS. Human peripheral blood mononuclear cells (PBMC) were isolated from whole blood using a standard density gradient centrifugation technique. Primary human T cells were isolated from PBMC using the Pan T-Cell Isolation Kit II (Miltenyi Biotec) and cultured in RPMI-1640 with 10% human serum (supplemented with nonessential amino acids, sodium pyruvate, glutamate, and HEPES) after isolation.

Binding experiments

Binding studies on $PSMA^+$ and $PSMA^-$ prostate cancer cell lines, human T cells, and CHO cell lines were performed using standard flow cytometry-based staining procedures (see Supplementary Methods). In a typical experiment, 300,000 cells per well were labeled with MOR209/ES414 or control molecules with concentrations ranging from 200 to 0.1 nmol/L in saline buffer with 0.2% BSA on ice, followed by washes and incubation with fluorescently-labeled secondary antibody (goat anti-human IgG, Life Technologies). After washing to remove excess secondary antibody, cells were incubated with 7-amino-actinomycin D (7-AAD; BD Biosciences) for 20 minutes then analyzed. Results were detected using either a BD LSRII or BD FACSCalibur flow cytometer and analyzed by FlowJo flow cytometry software (FlowJo, LLC). $7\text{-}AAD^+$ cells were excluded from analysis.

Cytotoxicity experiments

T-cell cytotoxicity induced by MOR209/ES414 was assessed by chromium-51 (^{51}Cr) release in 4-hour assays and high-content microscopy in multi-day assays. In a typical ^{51}Cr release assay, 2.5 million target cells were loaded with 0.125 mCi of ^{51}Cr and incubated for 75 minutes at 37°C, after which the cells were washed with media, resuspended in short-term assay media (RPMI + 10% FBS, nonessential amino acids, sodium pyruvate, 20 mmol/L HEPES) and dispensed at 10,000 cells per well into a 96-well U-bottom plate. Bispecific molecules were added at concentrations of 0.25 to 300 pmol/L, and isolated T cells were added to achieve a T-cell to target cell ratio of 5:1 or 10:1. NP-40 (0.4%) was used in control wells to achieve total lysis. Plates were incubated for 4 hours then centrifuged. Supernatants were transferred to a 96-well LumaPlate (PerkinElmer) and dried before radioactive decay was read on a PE Topcount scintillation counter. Percent specific lysis was calculated as: [(signal in drug treated sample−background signal from samples with T cells but no drug)/(signal in total lysis wells−background signal from samples with T cells but no drug)] × 100.

Longer-term cytotoxicity assays (up to 5 days) were performed using high-content microscopy. High-content microscopy assays were performed by culturing LNCaP(GFP) cells at 5,000 cells per well in a 96-well plate coated with poly-D-lysine (BD Biocoat, Corning) for 24 hours at 37°C with 5% CO_2 in RPMI + 10% FBS media. Culture media were replaced with long-term assay media [RPMI + 10% FBS, nonessential amino acids, sodium pyruvate, GlutaMAX supplement (Life Technologies), 55 μmol/L β-mercaptoethanol, 20 mmol/L HEPES] containing 50,000 isolated T cells for T-cell to target cell ratios of 10:1, and 100 pmol/L MOR209/ES414 was added. Replicate plates were prepared in parallel to provide multiple time points and incubated at 37°C with 5% CO_2 with one plate being removed every 24 hours for staining. For staining, media were changed to RPMI containing 1% FBS, 16.4 μmol/L Hoechst 33342 (Life Technologies), and 10 μg/mL 7-AAD. Cells were incubated for 30 minutes at 37°C then moved into a GE InCell Analyzer 1000 microscope for imaging. Total LNCaP(GFP) cell counts were collected from 12 fields per well using Hoechst stain for nuclear detection and GFP for cytoplasmic detection; $7\text{-}AAD^+$ LNCaP(GFP) cells were not included in cell counts. Specific mortality was calculated as 1-(live GFP^+ cells in well with drug present/live GFP^+ cells in well with no drug present).

Cytotoxicity assays at low E:T ratios

Following a similar protocol used to show serial lysis for other bispecific antibodies (19), primary T cells were cultured with Mitomycin C–treated PBMCs, phytohemagglutinin-L (PHA-L), and recombinant IL2 before use in cytotoxicity assays.

Mitomycin C treatment. PBMCs were resuspended after purification at 5×10^6 cells per mL with 25 μg/mL Mitomycin C (Sigma-Aldrich) in T-cell media (RPMI with 10% human serum, nonessential amino acids, sodium pyruvate, GlutaMAX supplement and 20 mmol/L HEPES). After 30-minute incubation at 37°C in 7% CO_2, cells were pelleted and washed 4 times with the same media. Mitomycin C–treated PBMCs were resuspended in T-cell media at 4 million/mL as feeder cells for PHA-L stimulation of T cells.

PHA-L stimulation. T cells were combined with Mitomycin C–treated PBMCs at a 1:2 ratio, and cultured for 5 days in the presence of 2 ng/mL IL2 (Peprotech) and 4 μg/mL PHA-L (Roche). Stimulated T cells were washed and cultured overnight in T-cell media + IL2 (2 ng/mL) before use in cytotoxicity assays.

Cytotoxicity assay. Target cells [LNCaP(GFP)] were cultured at 37°C with 5% CO_2 in RPMI + 10% FBS media, harvested with trypsin, and resuspended at 667,000 cells/mL in long-term assay media (RPMI + 10% FBS, nonessential amino acids, sodium pyruvate, GlutaMAX supplement, 55 μmol/L β-mercaptoethanol, and 20 mmol/L HEPES). Stimulated T cells were pelleted, resuspended in long-term assay media, mixed with approximately 50,000 target cells to reach effector to target cell ratios from 1:10 to 1:1 (150 μL), then dispensed into a 96-well plate coated with poly-D-lysine (BD Biocoat, Corning). MOR209/ES414 and media were added to bring the total volume to 200 μL/well. Each data point was run in triplicate. Plates were incubated for 24 hours at 37°C with 5% CO_2. After 24 hours, plates were centrifuged, media removed, wells washed with 200 μL PBS, centrifuged, media removed, and 0.4% NP-40 added. GFP

fluorescence was measured on a SpectraMax M3 plate reader (Molecular Devices) using an excitation wavelength of 485 nm and an emission wavelength of 538 nm. Specific mortality was calculated as 1−(fluorescence of well with drug present corrected for background/fluorescence of well with no drug present corrected for background).

T-cell proliferation and cytokine release assays

Induction of T-cell proliferation was assessed by labeling human PBMC with carboxyfluorescein diacetate succinimidyl ester (CFSE) and incubating them for 4 days at 37°C with 5% CO_2 with either bispecific molecules alone or with bispecific molecules and C4-2 ($PSMA^+$) target cells rendered nonproliferative by either Mitomycin C treatment or irradiation. Cells were plated at a PBMC to target cell ratio of 3:1, in RPMI with 10% human serum (Sigma-Aldrich). After 4 days, cell mixtures were incubated with 7-AAD and four fluorescently labeled antibodies [CD4-APC (BD Pharmingen), CD5-PE, CD8-Pacific Blue, CD25-PE-Cy7 (BioLegend)], washed, and analyzed in a BD LSRII flow cytometer. Data were analyzed using FlowJo software. Proliferation of live $CD4^+$ or $CD8^+$ T cells ($7AAD^-/CD5^+/CD4^+$ or $7AAD^-/CD5^+/CD8^+$) was assessed by reduction of CFSE fluorescence. Data were plotted as the percentage (average of two replicates) of T cells which had undergone at least one cell division.

For cytokine analysis, cultures of PBMCs, target cells, and bispecific molecules were plated and incubated as described above. Supernatants were collected at 4 or 24 hours. Supernatants were analyzed in a Milliplex MAP kit using a Bio-Plex 200 array reader following the manufacturer's protocol. Results represent the average of duplicate samples.

Mouse studies

Mice were purchased from the Jackson Laboratory and maintained under specific pathogen-free conditions. Harlan Teklad Rodent Diet 8656 and autoclaved deionized water were provided *ad libitum*. Mice were housed with a 12-hour light cycle in a facility meeting all Association for Assessment and Accreditation of Laboratory Animal Care specifications.

Pharmacokinetic analysis. Thirty male NOD/SCID γ (NOD.Cg-*Prkdc*^{scid} *Il2rg*^{tm1Wjl}/SzJ)(NSG) mice, approximately 7-week-old, received a single intravenous injection of 240 μg of MOR209/ES414 (approximately 10 mg/kg) in the lateral tail vein. Anesthetized mice were exsanguinated via cardiac puncture at 15 minutes and 2, 6, 24, 48, 72, 96, 168, 336, and 504 hours after injection. Serum was collected from 3 mice at each time point and frozen for later analysis.

Concentrations of MOR209/ES414 in sera were determined using an ELISA incorporating murine anti-idiotype antibodies specific for the N-terminal (1H5) and C-terminal (5H5) scFv regions. mAb 1H5 coated on plates captured MOR209/ES414, whereas mAb 5H5 conjugated to biotin detected bound MOR209/ES414. To quantify bound immune complexes from serum samples and assay controls, Streptavidin Poly-HRP (Pierce) and a fluorogenic peroxidase substrate were used, and results were read on a fluorescent plate reader. Serum samples, standards, and controls were incubated for 1 hour in coated and blocked plates, and additional incubation steps with mAb 5H5 biotin or streptavidin Poly-HRP were also for 1 hour at room temperature. Plates were washed between each ELISA step using a Biotek plate washer. The fluorogenic reaction was stopped after 20 minutes, and plates were read using excitation at 325 nm, and emission at 420 nm. Standard curves used to calculate serum concentrations consisted of various known concentrations of MOR209/ES414 spiked into assay diluent, fit with a 4-parameter logistic regression function in Molecular Devices SoftMax Pro software. Pharmacokinetic disposition parameters were estimated by noncompartmental analysis using Phoenix 64 with WinNonlin software (v6.4; Certara) set for intravenous bolus administration, uniform weighting, and sparse sampling.

Xenograft studies. NOD/SCID (NOD.CB17-*Prkdc*^{scid}/J) male mice between 6 and 8 weeks of age were obtained for two xenograft studies. In the first study, mice were coimplanted subcutaneously in the right flank with 2e6 C4-2B prostate tumor cells mixed with 1e6 human T cells in BD Matrigel Basement Matrix HC (BD Biosciences) on the day treatments were first administered. T cells were evaluated by flow cytometry to verify purity and characterize phenotypes before injection (Supplementary Methods; Supplementary Table S1). T cells from Donor 1 used in the C4-2B xenograft model were approximately 99.4% pure. T cells from Donor 2 used in the MDA-PCa-2b xenograft model were approximately 95.0% pure. Purified T cells from both donors were also phenotyped by flow cytometry by examining expression of CD45RA and CD62L (Supplementary Table S1). Both donors had a typical excess of $CD4^+$ T cells over $CD8^+$ T cells, and naïve T cells ($CD45RA^+$ $CD62L^+$) were the largest subset of both $CD4^+$ and $CD8^+$ T cells with each donor (Supplementary Table S1); however, there was a larger population of memory T cells in donor 2 compared with donor 1 (Supplementary Table S1). MOR209/ES414 was dosed intravenously on days 0, 4, and 8; the scFv-scFv comparator was dosed intravenously daily for the first 10 days. Mice were monitored for tumor volume and body weight loss endpoints for 148 days, defined as tumor volumes meeting or exceeding a volume of 1,500 mm^3, or 1,200 mm^3 if the next measurement would occur more than 2 days in the future, or a loss of more than 20% of the maximum body weight observed. Tumor volumes were calculated using the formula: volume = 0.5 [length × $(width)^2$]. In the second study, mice were coimplanted subcutaneously in the right flank with 2e6 MDA-PCa-2b prostate tumor cells mixed with 1e6 human T cells in Matrigel Matrix HC on the day therapeutic treatments were first administered. MOR209/ES414 was dosed intravenously on days 0, 4, and 8. Mice were monitored for tumor volume and body weight loss endpoints for 120 days. Serum draws to determine human PSA levels were taken at days 28, 42, 56, and 70. Serum PSA levels were quantified using a PSA assay kit from Meso Scale Discovery on an MSD SECTOR Imager 6000 (MSD). T cells were used without prior stimulation or expansion, and were isolated from a single human donor leukapheresis per study using a Pan T Cell Isolation Kit II and LS MACS Separation Columns (Miltenyi Biotec) or the Dynabeads Untouched Human T Cells Kit (Life Technologies).

Statistical analysis

Means, SDs, and SEs were calculated using Microsoft Excel software or GraphPad Prism software. Nonlinear regression analysis to determine EC_{50} values was performed using GraphPad Prism software. Tumor volumes in mouse tumor studies were compared using a one-way ANOVA for nonparametric data (Kruskal–Wallis test) with Dunn multiple comparisons post-test. Median survival of mice was analyzed using Kaplan–Meier

survival estimates with a log-rank test for comparing survival curves. Values of $P < 0.05$ were considered significant.

Results

Molecular design

MOR209/ES414 was constructed using the ADAPTIR platform and contains anti-PSMA scFvs linked to the CH2 and CH3 domains from human IgG1, connected to anti-CD3 scFvs by a flexible linker (Fig. 1A). Selection of the anti-CD3 scFv of MOR209/ES414 was based on functional screening of a series of anti-CD3 scFv domains in the ADAPTIR format to obtain a balance of efficient RTCC and T-cell proliferation activity. MOR209/ES414 forms a homodimer in solution through the IgG1 Fc region. Mutations were introduced into the lower hinge region and C-terminal region of the CH2 domain to prevent FcγR engagement and complement fixation, respectively, to prevent T-cell activation in absence of target cells. The structure of MOR209/ES414 differs from the structure of other bispecific antibody fragments such as tandem scFv molecules, which contain one scFv molecule specific for a target antigen linked by a short flexible linker to a second scFv molecule specific for CD3ε, without an IgG Fc region (Fig. 1B). A tandem scFv molecule specific for PSMA and CD3 based on BAY2010112 (16) was also constructed as a comparator; scFv domains in this molecule differ from those used in MOR209/ES414 and bind separate epitopes on PSMA and CD3ε.

Binding

Binding of MOR209/ES414 to human PSMA and CD3ε was quantified using flow cytometry. Binding of MOR209/ES414 was specific to prostate cancer cell lines expressing PSMA, such as C4-2B (EC_{50} of 4.0 nmol/L); no binding was observed to lines lacking PSMA, such as DU-145 (Fig. 1C). Binding of MOR209/ES414 to human CD3ε was measured by flow cytometry using PBMC obtained from multiple donors, as well as to human whole blood (Fig. 1D). MOR209/ES414 bound specifically to T cells in human PBMC with an EC_{50} of 1.99 nmol/L, and to T cells in human whole blood with an EC_{50} of 5.5 nmol/L. In both cases, no binding was observed on other cell subsets. Overall, MOR209/ES414 has similar affinities for PSMA and CD3ε, both of which are similar to those of the comparator tandem scFv (BAY2010112; ref. 16): affinities of the comparator scFv-scFv for CD3 and PSMA were 2.4 $\pm$ 0.62 nmol/L and 7.5 $\pm$ 1.1 nmol/L, respectively, on Jurkat and C4-2B cell lines. MOR209/ES414 binding to Fcγ receptors was tested on CHO cell lines expressing human Fcγ receptors (Supplementary Fig. S1A); no detectable binding was observed with MOR209/ES414 to any Fcγ receptor–expressing cell lines up to concentrations of 10 μmol/L.

Cytotoxicity

With unstimulated T cells, MOR209/ES414 induced substantial RTCC at low picomolar concentrations in multiple 4-hour chromium-51 release assays against $PSMA^+$ prostate cancer cells (LNCaP, C4-2B, MDA-PCa-2b, VCaP, and 22Rv1; Fig. 2A). To assess the relationship between PSMA cell surface density and the relative potency of MOR209/ES414, prostate tumor cell lines expressing varying levels of PSMA were treated with MOR209/ES414. Specific lysis was determined in short term chromium-51 release assays using a 5:1 excess of previously frozen, unstimulated T cells from a single donor. EC_{50} values measured by specific lysis did not vary significantly between the five $PSMA^+$ cell lines tested in these assays, suggesting PSMA density (within a 100-fold range) does not strongly impact cytotoxic activity induced by MOR209/ES414 (Fig. 2B; Supplementary Table S2). No specific lysis was observed against PSMA negative cell lines, such as DU-145, demonstrating that expression of PSMA is essential to elicit lysis. The relative ability of MOR209/ES414 to induce redirected T-cell lysis was compared directly with the tandem scFv in a 4-hour assay (Fig. 2C) using MDA-PCa-2b cells. Both MOR209/ES414 and the tandem scFv triggered similar levels of maximal specific lysis at saturating concentrations, but MOR209/ES414 showed activity at a substantially lower concentration (EC_{50} = 2.7 pmol/L) compared with the tandem scFv (EC_{50} = 99 pmol/L). Using multiple T-cell donors and $PSMA^+$-expressing cell lines, MOR209/ES414 exhibited EC_{50} values up to 30-fold lower than observed for the tandem scFv. These lower EC_{50} values observed for MOR209/ES414 may result from higher affinity binding to PSMA and possible binding avidity to target cells.

The EC_{50} values for MOR209/ES414 in 4-hour cytotoxicity assays with unstimulated T cells typically ranged from 1 to 30 pmol/L, depending on the blood donor, target cell line, and effector-to-target ratio; maximal specific lysis over 4 hours was typically 10% to 20%, similar to results seen with BiTE molecules (20). As part of its mechanism of action, MOR209/ES414 induces activation and proliferation of T cells, leading to an increased expression of cytolytic components such as granzymes and perforin. Both T-cell expansion and upregulation of cytolytic potential may enhance cytotoxicity observed during longer experiments. Survival of LNCaP(GFP) target cells was quantitated by high content microscopy over 120 hours of exposure to MOR209/ES414 and freshly isolated T cells. Primary, unstimulated T cells from four different donors were incubated with 100 pmol/L MOR209/ES414 and target LNCaP(GFP) cells at a 10:1 effector to target (E:T) cell ratio (Fig. 3A). Overall target cell mortality varied significantly between donors at 24 and 48 hours, but was similar for all donors (approaching 100%) at 120 hours. T-cell proliferation was also observed with every donor tested. These data suggest that T-cell activation and proliferation induced by MOR209/ES414 can enhance the cytotoxic activity of human T cells. To investigate whether or not T cells redirected by MOR209/ES414 can engage in multiple rounds of cytotoxicity against target cells (serial lysis), previously stimulated T cells were incubated at different E:T ratios with LNCaP(GFP) target cells and MOR209/ES414, similar to previous experiments demonstrating serial lysis from BiTE molecules (19). Over 24 hours, substantial target cell mortality was observed at all E:T ratios from 1:10 to 1:1 (Fig. 3B). At E:T ratios below 1:1, greater than stoichiometric mortality was observed, approximately 18% mortality at an E:T ratio of 1:10, 35% mortality at a ratio of 1:5, and 54% at a ratio of 1:3. Thus, individual T cells engaged by MOR209/ES414 can lyse multiple target cells.

T-cell proliferation

To characterize the effects of MOR209/ES414 on T-cell proliferation, PBMCs were labeled with CFSE to track cell division and incubated with MOR209/ES414 and target cells for 4 days. MOR209/ES414 induced proliferation of both $CD4^+$ and $CD8^+$ T cells in the presence of $PSMA^+$ target cells as assessed by multicolor flow cytometry (Fig. 4A). No proliferation was observed in the absence of $PSMA^+$ target cells (Fig. 4A) or in response to PSMA- cells (data not included). Similar results were observed in cultures using purified T cells instead of PBMCs.

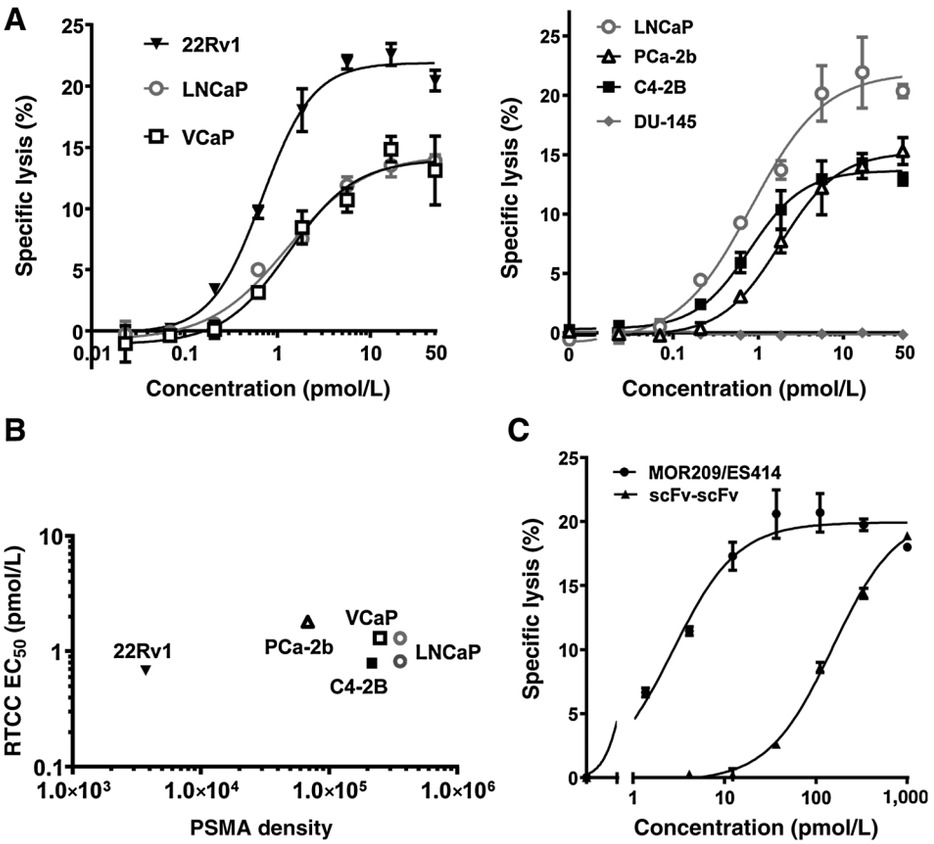

Figure 2.
A, specific lysis induced by MOR209/ES414 against six prostate cancer cell lines determined from chromium-51 release assay. Graphs represent two independent experiments performed on different dates. **B,** PSMA receptor expression plotted against EC_{50} values determined in **A**. **C,** specific lysis of MDA-PCa-2b cells induced by bispecific molecules determined from a chromium-51 release assay.

Compared with MOR209/ES414, the control tandem scFv molecule induced similar levels of $CD8^+$ T-cell proliferation and slightly higher $CD4^+$ T-cell proliferation (Fig. 4A). Multiple rounds of cell division were seen in both $CD4^+$ and $CD8^+$ T cells from loss of CFSE fluorescence, with the majority of $CD8^+$ T cells exhibiting four or more apparent divisions (Supplementary Fig. S1B and S1C). Fewer numbers of cell divisions were observed from $CD4^+$ T cells (Supplementary Fig. S1B and S1C). These results further confirm the robust and target-dependent nature of redirected T-cell responses mediated by MOR209/ES414.

Cytokine release

Activation of T cells through the TCR complex triggers secretion of cytokines within minutes, with cytokine release typically

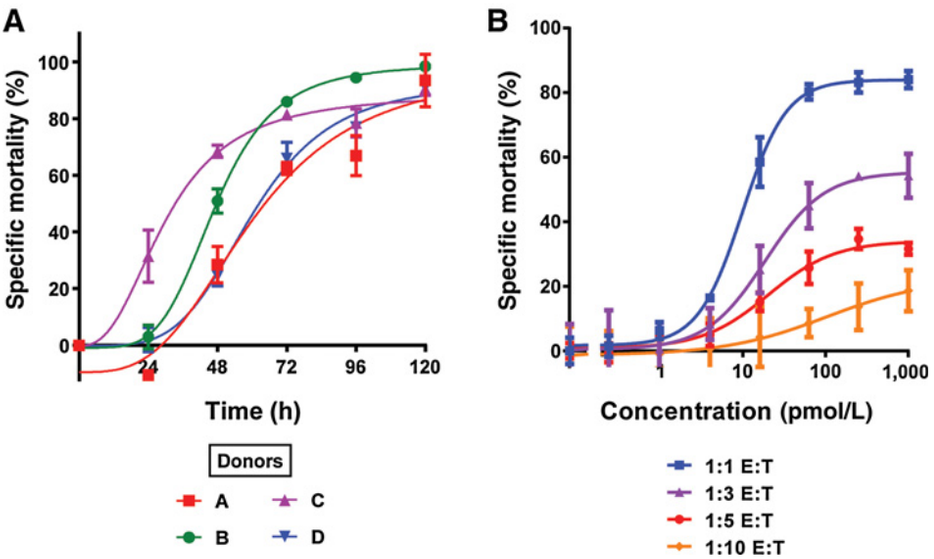

Figure 3.
A, specific mortality of LNCaP(GFP) cells using T cells from 4 donors shows donor-to-donor variation in initial kinetics of T-cell–directed lysis over time. **B,** specific mortality of LNCaP (GFP) cells at different ratios of effector to target cells induced by MOR209/ES414 over 24 hours.

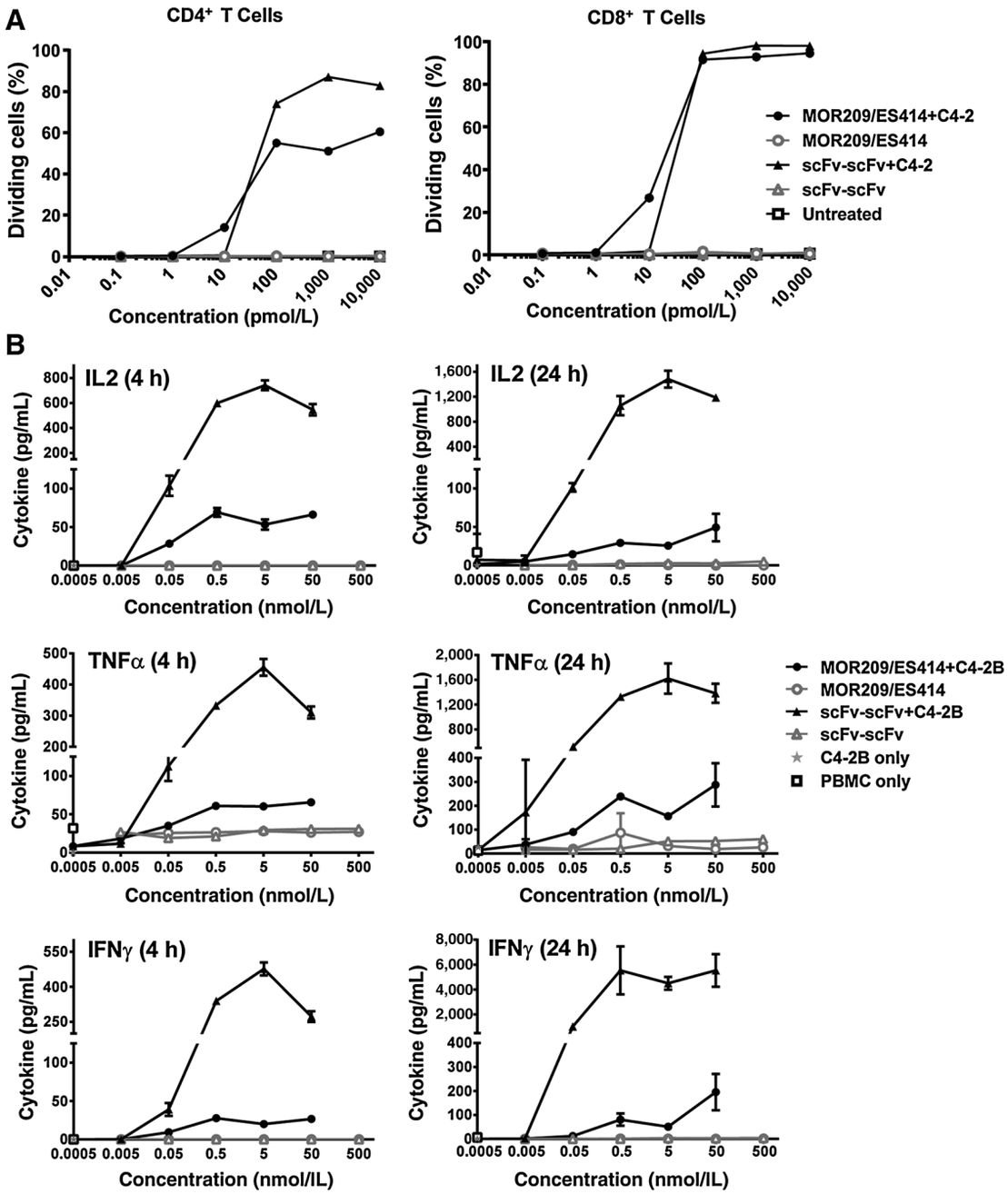

Figure 4.

A, purified human T cells were labeled with CFSE and incubated for 4 days at 37°C with bispecific proteins alone or with bispecific proteins and C4-2 ($PSMA^+$) cells. Data are plotted as the percentage of T cells that proliferated, as assessed by reduced CFSE fluorescence. **B,** PBMC were incubated for 4 or 24 hours at 37°C with bispecific proteins alone or with bispecific proteins and C4-2B ($PSMA^+$) cells. Cytokine levels were determined by Milliplex MAP analysis.

continuing for 2 to 96 hours (21, 22). In the blood, this first wave of T-cell–derived cytokines can stimulate cytokine secretion by other cell populations. The magnitude of the cytokine response correlates with the strength of the T-cell stimulus: strong T-cell activation leads to substantial cytokine release and T-cell proliferation, whereas weak or transient T-cell activation leads to a low level of cytokine release with little or no proliferation (23). In the clinic, drugs that induce strong T-cell activation and excessive cytokine release are associated with a series of adverse events, termed "cytokine release syndrome" (CRS). Because secreted cytokines can activate a systemic inflammatory response that can lead to life-threatening complications and limit drug administration, it is important to characterize the magnitude of cytokine production in response to molecules that activate T cells.

Cytokine secretion induced by MOR209/ES414 or the tandem scFv molecule was measured in whole PBMC cultures at 4 and 24 hours under conditions that lead to maximal T-cell activation and proliferation in the presence of $PSMA^+$ cells (Fig. 4B). Levels of various cytokines associated with T-cell activation were measured in supernatants using multiplexed analyte assays [e.g., IL2, IL4, IL5, IL6, IL8, IL10, IL12 (p40), IL13, IL17, TNFα, IFNγ, granulocyte-macrophage colony-stimulating factor (GM-CSF), and monocyte chemotactic protein-1 (MCP-1)]. No cytokines were detected after exposure to MOR209/ES414 in the absence of target cells at either time point. In the presence of $PSMA^+$ target cells, MOR209/ES414 induced low levels of IFNγ, TNFα, IL1β, IL2, IL4, IL6, IL10, IL13, IL17, and GM-CSF (Supplementary Fig. S2A). Increasing levels of cytokines were observed from the 4 to the 24-hour time points; examples generated from one individual donor are shown (Fig. 4B). Strikingly, the scFv-scFv molecule induced significantly higher levels of the same set of cytokines in the presence of $PSMA^+$ target cells when compared with MOR209/ES414 (Fig. 4B). This difference was observed at both 4 and 24 hours.

Together, these *in vitro* results demonstrate that MOR209/ES414 can induce efficient T-cell activation, RTCC, and proliferation in the presence of $PSMA^+$ target cells, while inducing relatively low levels of cytokine secretion in the process. The lower levels of cytokine production induced by MOR209/ES414 could result from the anti-CD3–binding domain used or the format of the molecule. To test this hypothesis, the anti-CD3 scFv of MOR209/ES414 was replaced with the anti-CD3 scFv of BAY2010112 to generate a control ADAPTIR molecule. When tested in the presence of target cells, the control ADAPTIR molecule induced comparable levels of T-cell activation as both the scFv-scFv and MOR209/ES414 (Supplementary Fig. S2B). However, the control molecule induced lower levels of cytokines than those induced by the tandem scFv and comparable with those induced by MOR209/ES414 (Supplementary Fig. S2C). This suggests that the limited cytokine release profile of MOR209/ES414 is a characteristic of the anti-PSMA x anti-CD3 ADAPTIR format.

Pharmacokinetic analysis

Pharmacokinetic analysis of MOR209/ES414 was conducted in immunodeficient mice to model conditions for xenograft studies. Normal male NSG mice were injected intravenously with a 240 μg bolus dose of MOR209/ES414, equivalent to approximately 10 mg/kg. Serum concentrations were determined for MOR209/ES414 using ELISA methods. Estimated PK parameters are shown in Table 1. The apparent terminal elimination half-life of MOR209/ES414 was approximately 96.5 hours, and clearance and volume of distribution estimates were 5.43 mL/hour/kg and 756 mL/kg, respectively. Because the volume of distribution had a high value indicative of extensive distribution throughout tissues, serum samples were also analyzed using compartmental analysis with a precompiled two-compartment model for bolus intravenous dosing (data not shown). Mean half-life and volume of distribution parameters were similar between models, suggesting MOR209/ES414 distributes extensively throughout tissues.

***In vivo* xenograft studies**

The ability of MOR209/ES414 to prevent tumor growth *in vivo* was evaluated in two xenograft models of prostate cancer (C4-2B and MDA-PCa-2b) in NOD/SCID mice using adoptively transferred human T cells, similar to previous studies using bispecific antibody fragments (15, 16). The ability of MOR209/ES414 to prevent growth of C4-2B tumors was compared with the tandem scFv control. Both molecules were administered intravenously. Doses of 0.3 μg to 30 μg MOR209/ES414 (approximately 0.015–1.5 mg/kg) were administered on days 0, 4, and 8. On the basis of its reported shorter serum half-life (16), the tandem scFv control was dosed daily from day 0 to day 10 at 5 μg (0.25 mg/kg). Tumor growth was monitored for 148 days. Transient swelling at the site of tumor implantation was observed in all groups, including controls, and was included in tumor-site measurements. In the absence of tumors, this swelling resolved by day 55. MOR209/ES414 exhibited inhibitory effects on outgrowth of C4-2B tumors at all doses in the presence of coimplanted human T cells (Fig. 5A), but no inhibition of tumor growth was seen in animals dosed with MOR209/ES414 in the absence of human T cells. For groups coimplanted with C4-2B and human effector cells, mean tumor volumes of each MOR209/ES414-treated group on day 48 were significantly lower than that of the T-cell + vehicle control group ($P < 0.01$). The tandem scFv control also inhibited C4-2B tumor growth ($P < 0.01$) Survival of mice treated with any of the MOR209/ES414 dose regimens or the tandem scFv control in the presence of human T cells was significantly prolonged relative to all control groups ($P = 0.0046$ to <0.0001; Fig. 5B, Supplementary Tables S3 and S4). At the end of the study, 3 of 15 mice treated with the tandem scFv were alive and tumor free, and 6 of 15 mice treated with 3 μg, and 1 of 15 mice treated with 30 μg of MOR209/ES414 were tumor free.

In the second model, the ability of MOR209/ES414 to prevent growth of MDA-PCa-2b tumors was assessed using a similar dose titration (0.3 to 30 μg/dose) and dosing frequency (intravenous doses on days 0, 4, and 8). MOR209/ES414 also exhibited significant inhibitory effects on the outgrowth of MDA-PCa-2b tumors at all doses tested in the presence of coimplanted human T cells (Fig. 5C) compared with the vehicle control group ($P = 0.0006$ to $P < 0.0001$). As with the C4-2B model, no inhibitory effect on the outgrowth of MDA-PCa-2b tumors was observed in control mice treated with MOR209/ES414 in the absence of

Table 1. Estimated pharmacokinetic disposition parameters of MOR209/ES414 after intravenous administration in mice

Parameter	Units	Estimates determined by ELISA
HL	h	96.5
T_{max}	h	0.25
C_{max}	μg/mL	96.24
C_{max}/D	kg*μg/mL/mg	9.6
AUCINF	h*μg/mL	1,847.5
AUCINF/D	h*kg*μg/mL/mg	184.2
Vz	mL/kg	755.6
CL	mL/h/kg	5.43
Vss	mL/kg	469.2

NOTE: Serum levels of MOR209/ES414 after a single intravenous bolus administration of 10 mg/kg were determined and used to derive pharmacokinetic parameters.

Abbreviations: AUCINF, area under the curve from the time of dosing extrapolated to infinity; AUCINF/D, AUCINF normalized by dose; C_{max}, maximum observed concentration, occurring at T_{max}; C_{max}/D, maximum observed concentration divided by dose; CL, serum clearance; HL, apparent terminal elimination half-life; T_{max}, time of maximum observed concentration; Vz, volume of distribution based on the terminal phase; Vss, volume of distribution at steady state.

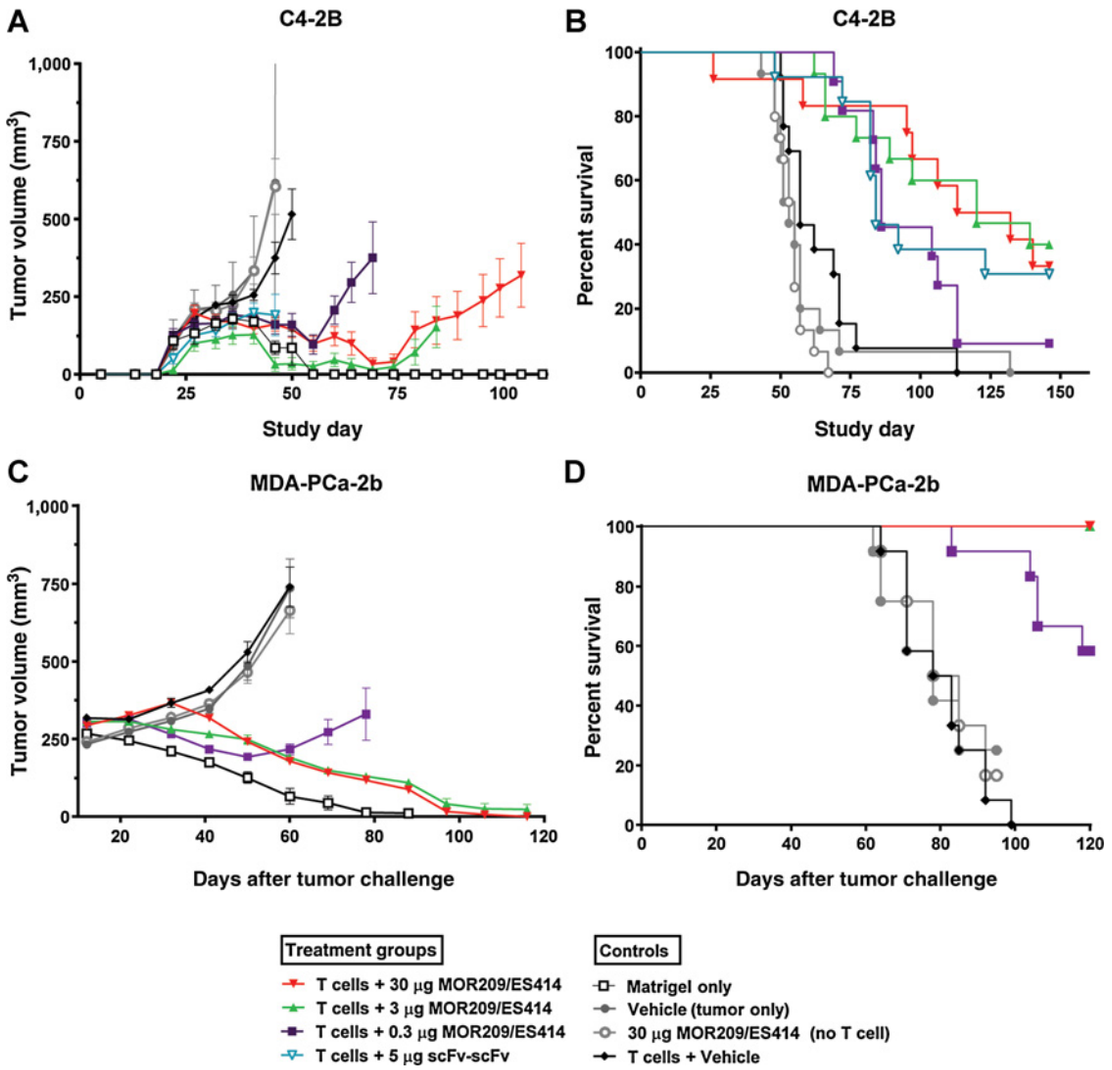

Figure 5.

Inhibition of prostate cancer xenografts by MOR209/ES414. Tumor volumes are plotted as means with SE; curves are plotted until the first mouse in each group reached a tumor volume endpoint. In the C4-2B model, tumor volumes of mice reaching weight loss endpoints were carried forward in the plotted means. **A,** tumor volumes in the C4-2B model. **B,** overall survival in the C4-2B model. **C,** tumor volumes in the MDA-PCa-2b model. **D,** overall survival in the MDA-PCa-2b model.

human T cells. Treatment with any of the MOR209/ES414 dose regimens in the presence of coimplanted human T cells significantly prolonged the survival of mice relative to all control groups (Fig. 5D; $P < 0.0001$). Owing to the low tumor incidence in the treated groups, human PSA levels in serum were used to assess residual tumor burden in the MDA-PCa-2b model (Supplementary Fig. S3). Serum samples were collected on days 28, 42, 56, and 70 and quantified using electrochemiluminesence. All dose groups showed a statistically significant decrease in serum PSA levels compared with the vehicle control group, with animals in the 3 and 30 μg dose cohorts demonstrating no measureable serum PSA at day 56, suggesting minimal tumor burden in these mice. Interim PSA results were confirmed at the end of the study when 2/12, 10/12, and 12/12 mice in the 0.3, 3, and 30 μg dose cohorts, respectively, were tumor free.

Discussion

Redirection of T-cell cytotoxicity by bispecific antibody fragments has been demonstrated to be clinically effective, as exemplified by the recent FDA approval of blinatumomab (Blincyto, Amgen) for the treatment of relapsed or refractory acute lymphoblastic leukemia. Although this class of molecules has shown substantial activity in clinical trials, two drawbacks limit their use as therapeutics. First, a short serum elimination half-life requires antibody fragments to be either administered through continuous infusion from an ambulatory infusion pump or injected daily. However, in the event of serious toxicity, ceasing administration does provide a rapid route to removing these drugs from the system. Second, high levels of cytokine release triggered from T-cell

activation require premedication with immunosuppressive drugs such as dexamethasone (24, 25) and close monitoring for immune-related toxicities, such as CRS and hemophagocytic lymphohistiocytosis (26). These drawbacks impact the dosing and overall exposure that can be achieved with these molecules.

An ideal "second-generation" bispecific antibody molecule would maintain the desirable characteristics of bispecific antibody fragments, target-dependent redirection of T-cell cytotoxicity, extended target-dependent T-cell activation and proliferation, with a prolonged serum half-life and a reduced cytokine release profile. However, the path to generating such a molecule is not straightforward. Fusion of antibody fragments to antibody Fcγ regions has been shown to improve serum half-lives, but antibody Fcγ domains can also bind to an array of Fcγ receptors on a variety of cells. This can result in unintentional T-cell activation in a mixed lymphocyte population or in blood and possible additional toxicities resulting from non-specific cytokine release and cytotoxicity against normal lymphocytes. In addition, immunotherapeutics with an extended serum half-life offer the potential for adverse events of extended duration.

The ADAPTIR platform was used to engineer MOR209/ES414, which redirects T-cell cytotoxicity and activation against $PSMA^+$ target cells, with an extended serum half-life and minimal cytokine release *in vitro*. To our knowledge, this is the first report of a bispecific antibody with these characteristics. MOR209/ES414 contains a modified Fc domain that does not bind FcγRs and binds selectively to T cells and PSMA-expressing target cells via the scFv-binding domains. MOR209/ES414's design enables efficient induction of target-dependent cell lysis and T-cell proliferation over multiple days in the presence of only moderate levels of cytokine release when PSMA target is present. After exposure to MOR209/ES414, $CD8^+$ T cells showed robust target-dependent proliferation, but a reduced degree of proliferation was seen from $CD4^+$ T cells, which are predominantly responsible for cytokine production (27). The resulting limited cytokine release could arise from the structure of the ADAPTIR format, which may attenuate the degree of TCR stimulation compared with other bispecific antibody formats. In *in vitro* studies, cytotoxic activity is comparable with previously described bispecific antibody fragments targeting PSMA and CD3. Importantly, these results indicate that high levels of cytokine release are not necessary to sustain a cytotoxic T-cell response. In *in vivo* studies, MOR209/ES414 significantly inhibited tumor growth and significantly increased survival when compared with vehicle controls. This effect was comparable with previously described antibody fragments; however, MOR209/ES414 does not require daily administration to show activity. These promising preclinical studies warrant further investigation of MOR209/ES414 as a novel immunotherapeutic approach for the treatment of mCRPC.

Disclosure of Potential Conflicts of Interest

T. Sewell has ownership interest in Emergent BioSolutions stock. J. Bannink has ownership interest in stock of Emergent BioSolutions. R.A. Chenault has ownership interest (including patents) in Emergent BioSolutions Inc. D. Bienvenue has ownership interest (including patents) in Emergent BioSolutions. C.J. McMahan has ownership interest (including patents) in Emergent BioSolutions. S.K. Natarajan has ownership interest (including patents) in Emergent BioSolutions (Patents). J.A. Gross has ownership interest (including patents) in Emergent BioSolutions. J.W. Blankenship has ownership interest (including patents) in Emergent BioSolutions. No potential conflicts of interest were disclosed by the other authors.

Authors' Contributions

Conception and design: R.E. Miller, P.A. Algate, C.J. McMahan, S.K. Natarajan, J.A. Gross, J.W. Blankenship

Development of methodology: G. Hernandez-Hoyos, T. Sewell, R.A. Chenault, J. Wiens, P.A. Algate, S.K. Natarajan, J.A. Gross

Acquisition of data (provided animals, acquired and managed patients, provided facilities, etc.): G. Hernandez-Hoyos, T. Sewell, R. Bader, J. Bannink, M. Daugherty, M. Dasovich, H. Fang, R. Gottschalk, J. Kumer, R.E. Miller, P. Ravikumar, J. Wiens, D. Bienvenue, C.J. McMahan, J.A. Gross

Analysis and interpretation of data (e.g., statistical analysis, biostatistics, computational analysis): G. Hernandez-Hoyos, T. Sewell, R. Bader, J. Bannink, R.A. Chenault, M. Daugherty, H. Fang, R. Gottschalk, J. Kumer, P. Ravikumar, J. Wiens, P.A. Algate, C.J. McMahan, J.A. Gross, J.W. Blankenship

Writing, review, and/or revision of the manuscript: G. Hernandez-Hoyos, J. Bannink, R.A. Chenault, M. Daugherty, R.E. Miller, P. Ravikumar, J. Wiens, P.A. Algate, D. Bienvenue, C.J. McMahan, J.A. Gross, J.W. Blankenship

Administrative, technical, or material support (i.e., reporting or organizing data, constructing databases): R. Bader, J. Wiens, D. Bienvenue

Study supervision: C.J. McMahan, S.K. Natarajan, J.A. Gross, J.W. Blankenship

Other (designed, performed, analyzed, and interpreted experimental work not involved in molecule design and protein expression): G. Hernandez-Hoyos

Acknowledgments

The authors also would like to acknowledge the assistance of M. Blake and A. Eisenfeld with article preparation and review, M. Aguilar with protein purification, and K. Bannink, J. Lambie, and W. Bhartso of the animal research facility with additional support for the mouse studies.

The costs of publication of this article were defrayed in part by the payment of page charges. This article must therefore be hereby marked *advertisement* in accordance with 18 U.S.C. Section 1734 solely to indicate this fact.

Received March 30, 2015; revised June 6, 2016; accepted June 14, 2016; published OnlineFirst July 12, 2016.

References

1. Tannock IF, de Wit R, Berry WR, Horti J, Pluzanska A, Chi KN, et al. Docetaxel plus prednisone or mitoxantrone plus prednisone for advanced prostate cancer. New Engl J Med 2004;351:1502–12.
2. de Bono JS, Logothetis CJ, Molina A, Fizazi K, North S, Chu L, et al. Abiraterone and increased survival in metastatic prostate cancer. New Engl J Med 2011;364:1995–2005.
3. Scher HI, Fizazi K, Saad F, Taplin ME, Sternberg CN, Miller K, et al. Increased survival with enzalutamide in prostate cancer after chemotherapy. New Engl J Med 2012;367:1187–97.
4. de Bono JS, Oudard S, Ozguroglu M, Hansen S, Machiels JP, Kocak I, et al. Prednisone plus cabazitaxel or mitoxantrone for metastatic castration-resistant prostate cancer progressing after docetaxel treatment: a randomised open-label trial. Lancet 2010;376:1147–54.
5. Garcia JA, Rini BI. Castration-resistant prostate cancer: many treatments, many options, many challenges ahead. Cancer 2012;118:2583–93.
6. Quinn DI, Shore ND, Egawa S, Gerritsen WR, Fizazi K. Immunotherapy for castration-resistant prostate cancer: progress and new paradigms. Urol Oncol 2015;33:245–60.
7. Chang SS. Overview of prostate-specific membrane antigen. Rev Urol 2004;6Suppl 10:S13–8.
8. O'Keefe DS, Bacich DJ, Heston WDW. Prostate specific membrane antigen. In: Chung LWK, Isaacs WB, Simons JW, editors. Prostate cancer: biology,

genetics and the new therapeutics. Totowa, NJ: Humana Press; 2001. p.307–26.
9. Wolf P. Prostate specific membrane antigen as biomarker and therapeutic target for prostate cancer. In: Spiess PE, editor. Prostate cancer—diagnostic and therapeutic advances. Munich, Germany: InTech; 2011. p.81–100.
10. Hinkle GH, Burgers JK, Neal CE, Texter JH, Kahn D, Williams RD, et al. Multicenter radioimmunoscintigraphic evaluation of patients with prostate carcinoma using indium-111 capromab pendetide. Cancer 1998;83:739–47.
11. Milowsky MI, Nanus DM, Kostakoglu L, Vallabhajosula S, Goldsmith SJ, Bander NH. Phase I trial of yttrium-90-labeled anti–prostate-specific membrane antigen monoclonal antibody J591 for androgen-independent prostate cancer. J Clin Oncol 2004;22:2522–31.
12. Bander NH, Milowsky MI, Nanus DM, Kostakoglu L, Vallabhajosula S, Goldsmith SJ. Phase I trial of 177lutetium-labeled J591, a monoclonal antibody to prostate-specific membrane antigen, in patients with androgen-independent prostate cancer. J Clin Oncol 2005;23:4591–601.
13. Vallabhajosula S, Kuji I, Hamacher KA, Konishi S, Kostakoglu L, Kothari PA, et al. Pharmacokinetics and biodistribution of 111In- and 177Lu-labeled J591 antibody specific for prostate-specific membrane antigen: prediction of 90Y-J591 radiation dosimetry based on 111In or 177Lu? J Nucl Med 2005;46:634–41.
14. Galsky MD, Eisenberger M, Moore-Cooper S, Kelly WK, Slovin SF, DeLa-Cruz A, et al. Phase I trial of the prostate-specific membrane antigen-directed immunoconjugate MLN2704 in patients with progressive metastatic castration-resistant prostate cancer. J Clin Oncol 2008;26:2147–54.
15. Buhler P, Wolf P, Gierschner D, Schaber I, Katzenwadel A, Schultze-Seemann W, et al. A bispecific diabody directed against prostate-specific membrane antigen and CD3 induces T-cell mediated lysis of prostate cancer cells. Cancer Immunol Immunother 2008;57:43–52.
16. Friedrich M, Raum T, Lutterbuese R, Voelkel M, Deegen P, Rau D, et al. Regression of human prostate cancer xenografts in mice by AMG 212/BAY2010112, a novel PSMA/CD3-bispecific BiTE antibody cross-reactive with non-human primate antigens. Mol Cancer Ther 2012;11:2664–73.
17. Wolf E, Hofmeister R, Kufer P, Schlereth B, Baeuerle PA. BiTEs: bispecific antibody constructs with unique anti-tumor activity. Drug Discov Today 2005;10:1237–44.
18. World Health Organization. Proposed International Nonproprietary Names: List 111. WHO Drug Information 2014;28:251–2.
19. Hoffmann P, Hofmeister R, Brischwein K, Brandl C, Crommer S, Bargou R, et al. Serial killing of tumor cells by cytotoxic T cells redirected with a CD19-/CD3-bispecific single-chain antibody construct. Int J Cancer 2005;115:98–104.
20. Loffler A, Kufer P, Lutterbuse R, Zettl F, Daniel PT, Schwenkenbecher JM, et al. A recombinant bispecific single-chain antibody, CD19 x CD3, induces rapid and high lymphoma-directed cytotoxicity by unstimulated T lymphocytes. Blood 2000;95:2098–103.
21. McHugh S, Deighton J, Rifkin I, Ewan P. Kinetics and functional implications of Th1 and Th2 cytokine production following activation of peripheral blood mononuclear cells in primary culture. Eur J Immunol 1996;26:1260–5.
22. Kum WW, Cameron SB, Hung RW, Kalyan S, Chow AW. Temporal sequence and kinetics of proinflammatory and anti-inflammatory cytokine secretion induced by toxic shock syndrome toxin 1 in human peripheral blood mononuclear cells. Infect Immun 2001;69:7544–9.
23. Corse E, Gottschalk RA, Allison JP. Strength of TCR-peptide/MHC interactions and *in vivo* T-cell responses. J Immunol 2011;186:5039–45.
24. Blincyto [package insert]. Thousand Oaks, CA: Amgen Inc.
25. Nagorsen D, Kufer P, Baeuerle PA, Bargou R. Blinatumomab: a historical perspective. Pharm Thera 2012;136:334–42.
26. Teachey DT, Rheingold SR, Maude SL, Zugmaier G, Barrett DM, Seif AE, et al. Cytokine release syndrome after blinatumomab treatment related to abnormal macrophage activation and ameliorated with cytokine-directed therapy. Blood 2013;121:5154–7.
27. Rabenstein H, Behrendt AC, Ellwart JW, Naumann R, Horsch M, Beckers J, et al. Differential kinetics of antigen dependency of $CD4^+$ and $CD8^+$ T cells. J Immunol 2014;192:3507–17.